

# Fermi National Accelerator Laboratory

FERMILAB-Conf-83/76-EXP  
7420.616

## MEASUREMENT OF $\sin^2\theta_w$ IN SEMILEPTONIC $\nu$ Fe AND $\bar{\nu}$ Fe INTERACTIONS\*

R. E. Blair, D. B. MacFarlane, R. L. Messner,  
D. B. Novikoff, and M. V. Purohit  
California Institute of Technology, Pasadena, California 91125

F. S. Merritt and P. G. Reutens  
University of Chicago, Chicago, Illinois 60637

F. J. Sciulli and M. H. Shaevitz  
Columbia University, New York, New York 10027

D. Edwards, H. T. Edwards, H. E. Fisk, Y. Fukushima, B. N. Jin,  
Q. A. Kerns, T. Kondo, P. A. Rapidis, S. L. Segler, R. J. Stefanski,  
D. E. Theriot, and D. D. Yovanovitch  
Fermi National Accelerator Laboratory, Batavia, Illinois 60510

A. Bodek, R. N. Coleman, and W. L. Marsh  
University of Rochester, Rochester, New York 14627

and

O. D. Fackler and K. A. Jenkins  
Rockefeller University, New York, New York 10021

October 1983

\*Presented by P. A. Rapidis at the Europhysics Study Conference on Electroweak Effects at High Energies, Erice, Italy, February 1-12, 1983.

# MEASUREMENT OF $\sin^2\theta_w$ IN SEMILEPTONIC

## $\nu$ Fe AND $\bar{\nu}$ Fe INTERACTIONS

R.E. Blair<sup>1</sup>, A. Bodek<sup>5</sup>, R.N. Coleman<sup>5</sup>, D. Edwards<sup>4</sup>, H.T. Edwards<sup>4</sup>,  
O.D. Fackler<sup>6</sup>, H.E. Fisk<sup>4</sup>, Y. Fukushima<sup>4</sup>, K.A. Jenkins<sup>6</sup>,  
B.N. Jin<sup>4</sup>, Q.A. Kerns<sup>4</sup>, T. Kondo<sup>4</sup>, D.B. MacFarlane<sup>1</sup>,  
W.L. Marsh<sup>5</sup>, F.S. Merritt<sup>2</sup>, R.L. Messner<sup>1</sup>, D.B. Novikoff<sup>1</sup>,  
M.V. Purohit<sup>1</sup>, P.A. Rapidis<sup>4</sup>, P.G. Reutens<sup>2</sup>, F.J. Sciulli<sup>3</sup>,  
S.L. Segler<sup>4</sup>, M.H. Shaevitz<sup>3</sup>, R.J. Stefanski<sup>4</sup>, D.E. Theriot<sup>4</sup>,  
D.D. Yovanovitch<sup>4</sup>

<sup>1</sup> California Institute of Technology, Pasadena, CA 91125

<sup>2</sup> University of Chicago, Chicago, IL 60637

<sup>3</sup> Columbia University, New York, NY 10027

<sup>4</sup> Fermi National Accelerator Laboratory, Batavia, IL 60510

<sup>5</sup> University of Rochester, Rochester, NY 14627

<sup>6</sup> Rockefeller University, New York, NY 10021

Presented by P.A. Rapidis\*

We report results from neutral current scattering of muon neutrinos and antineutrinos on iron nuclei by the CCFRR experiment at Fermilab. Our objective is the measurement of  $\sin^2\theta_w$  from inclusive semileptonic neutrino-nucleon interactions. Such a measurement, even though it is subject to more corrections than the analogous measurement in neutrino-electron scattering (e.g. due to the presence of a strange quark sea in the nucleon), has a high degree of statistical accuracy and may afford the most precise test of the standard model of electro-weak interactions. Furthermore, the recent observations<sup>1</sup> of the  $Z^0$  and  $W^\pm$  in proton-antiproton collisions give such a measurement added topical interest. The comparison of  $\sin^2\theta_w$  determined from the masses of the  $Z^0$  and  $W^\pm$  and from neutrino interactions, i.e. from different processes and energy regions, may hold some surprises. Finally, the grand-unified theories make definite predictions<sup>2</sup> about the value of  $\sin^2\theta_w$  and the lifetime of the proton;  $\sin^2\theta_w$  measurements test the validity of these theories.

The experiment was performed in Fermilab's dichromatic neutrino beam and utilized a large detector consisting of an iron-scintillator target calorimeter followed by a steel toroidal muon spectrometer. Since the detector and beamline have been described elsewhere<sup>3</sup> we will only give a short description.

Briefly, 400 GeV protons impinge on a BeO target and produce secondary particles which are momentum and sign selected by a point-to-parallel beam channel. The secondary particles include e,  $\pi$ , K, and p's with an rms momentum spread of 10% and an rms angular

---

\* Presented at the Europhysics Study Conference on Electroweak Effects at High Energies, February 1-12, 1983, Erice, Italy.

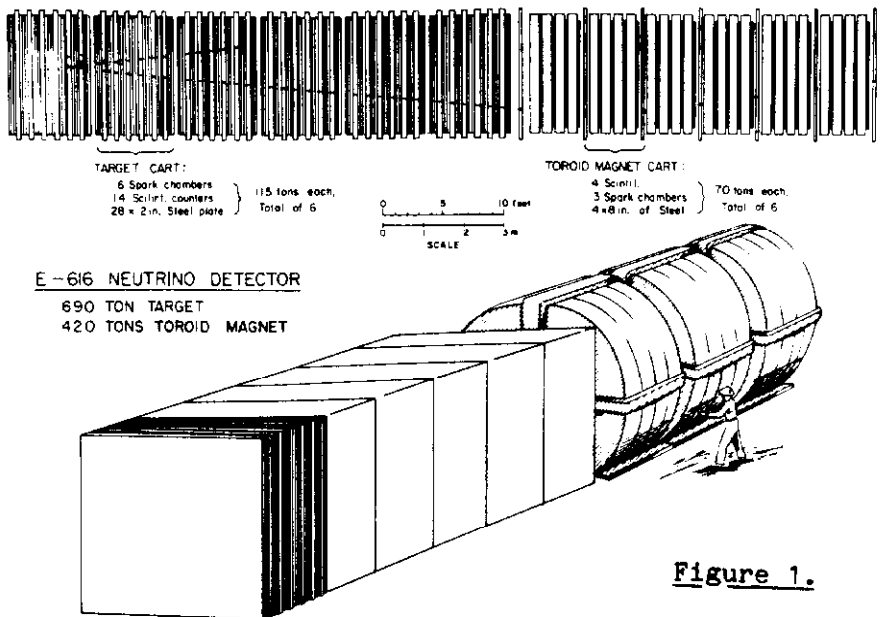


Figure 1.

width of approximately 0.15 mrad. These secondaries travel through a 340m long evacuated decay space where some of the  $\pi$ 's and K's decay and produce neutrinos and muons. A beam dump at the end of the decay region and a 900m long steel and earth shield absorb the surviving secondaries and the decay muons. Instrumentation in the beam line measures the intensity and particle composition of the secondary beam and allows us to calculate the neutrino flux at the end of the shield where our detector is located. Data were taken at five settings of the secondary beam momentum with both polarities.

The detector (Fig. 1) is a hadron calorimeter made of 690 tons of steel plates interspersed with spark chambers (every 20cm of steel) and liquid scintillation counters (every 10cm of steel). It is followed by a steel toroidal spectrometer instrumented with spark chambers (every 80cm of steel) and scintillation counters (every 20cm of steel). Hadron energies and muon emission angles are measured in the calorimeter, and muon momenta are reconstructed in the spectrometer. The hadronic shower energy is measured with an rms resolution of

$$\Delta E_H = 0.89 \sqrt{E_H} (\text{GeV})$$

The sparks in a hadronic shower can be used to determine the transverse position of the event vertex with an energy independent rms resolution of 1.7 inches. Even though the vertex for charged current events with a final state muon can be determined much more

precisely, the charged current and neutral current events were treated in an identical fashion and only the vertex determined by the hadronic shower information was used. Calibration data taken with pions of known energy show that the maximum length for hadronic showers in our calorimeter for energies up to 200 GeV is 210 cm of steel.

Three types of event triggers were installed :

- i. The muon trigger requiring a particle to penetrate through part of the calorimeter and the upstream part of the spectrometer; no hadronic energy requirement was imposed.
- ii. The penetration trigger requiring the deposition of at least 4 GeV of energy in the calorimeter and the presence of a penetrating particle (muon) travelling through 160 cm of steel or more.
- iii. The hadronic energy trigger requiring only an energy deposition of 12 GeV in the calorimeter.

Events of the first two triggers were used for the study of charged current interactions<sup>4</sup> and of trigger and reconstruction efficiencies for events that also satisfied the hadronic energy trigger. From such studies we have determined that for hadronic energies greater than 18 GeV the hadronic trigger is 100% efficient. The events used in this analysis were required to satisfy the hadronic energy trigger, have a minimum hadronic energy of 20 GeV, and have a vertex within a 40 inch radius from the center of the detector.

The traditional technique<sup>5</sup> of determining  $\sin^2\theta_w$  is based on the study of the cross-section ratios

$$R_\nu = \frac{\sigma_\nu^{NC}}{\sigma_\nu^{CC}} \quad , \text{ and } \quad R_{\bar{\nu}} = \frac{\sigma_{\bar{\nu}}^{NC}}{\sigma_{\bar{\nu}}^{CC}} \quad .$$

The precision of the determined  $\sin^2\theta_w$  depends on the precision with which one can measure  $R_\nu$  and  $R_{\bar{\nu}}$ . In determining these ratios one has to estimate the number of neutral current events in the presence of backgrounds due to misidentified charged current events.

Neutral current events are identified through the study of the length distribution of events where the length of the event refers to the distance over which energy is deposited in the target calorimeter. Charged current interactions, besides producing a relatively short hadronic shower at the event vertex, are accompanied by a final state muon that travels many meters in our steel target, and therefore, have a long event length. Neutral current interactions give rise to events with short lengths since the final state contains only hadrons. The major problem in determining  $R_\nu$  and  $R_{\bar{\nu}}$  arises from charged current events where the

muon is produced at a large angle and leaves the calorimeter from the side after a short distance. These events can be easily misidentified as neutral current events. Such backgrounds are approximately 20% of the neutral current interactions (Fig. 2a).

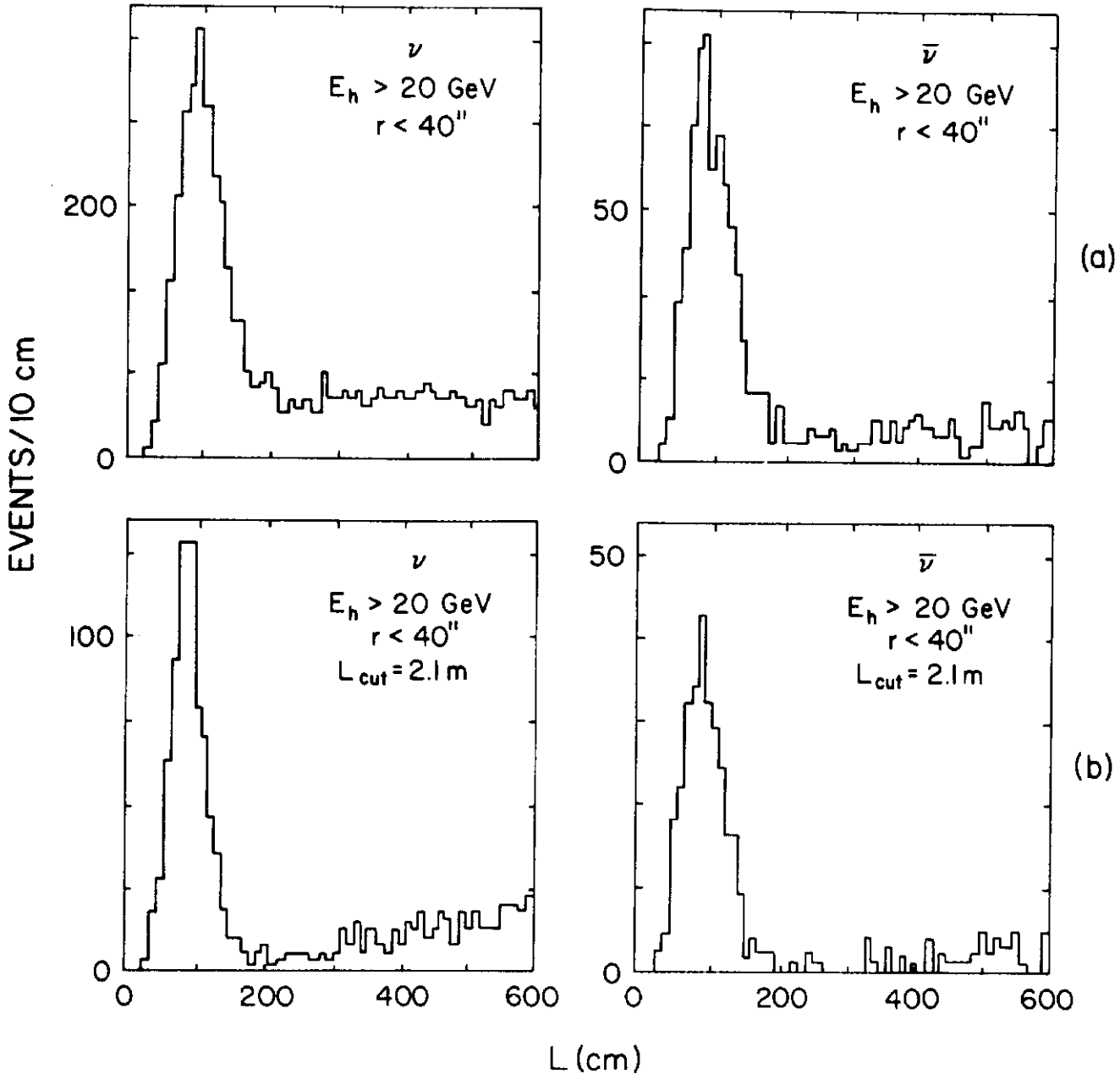


Figure 2. Length distribution for (a) events satisfying the trigger, hadronic energy, and radius requirements, (b) events that in addition satisfy the requirement  $y_{NC} < y_{cut}$ . The data shown here and in Figures 4 and 5 were obtained for a secondary beam momentum of 200 GeV/c. They correspond to approximately 25% of the full data sample.

A different method has been proposed by Paschos and Wolfenstein<sup>6</sup>, who suggest using the ratios :

$$R_- = \frac{\frac{d^2\sigma_{\nu}^{NC}}{dx dy} - \frac{d^2\sigma_{\bar{\nu}}^{NC}}{dx dy}}{\frac{d^2\sigma_{\nu}^{CC}}{dx dy} - \frac{d^2\sigma_{\bar{\nu}}^{CC}}{dx dy}} = \rho^2 \left( \frac{1}{2} - \sin^2\theta_w \right) \quad \text{and}$$

$$R_+ = \frac{\frac{d^2\sigma_{\nu}^{NC}}{dx dy} + \frac{d^2\sigma_{\bar{\nu}}^{NC}}{dx dy}}{\frac{d^2\sigma_{\nu}^{CC}}{dx dy} + \frac{d^2\sigma_{\bar{\nu}}^{CC}}{dx dy}} = \rho^2 \left( \frac{1}{2} - \sin^2\theta_w + \frac{10}{9} \sin^4\theta_w \right),$$

These ratios are valid over any region of x and y; using them allows us to restrict our attention to particular regions in y where the separation between neutral current interactions and charged current interactions is clear. Furthermore, R being in essence the ratio of two non-singlet structure functions, is largely independent of the quark sea component of the target nucleons.

The following procedure was used to limit the y region in our analysis. A scan of the data was used to determine the minimum event length in the target,  $L_{cut}$ , necessary for the muon to be recognized efficiently.  $L_{cut}$  was determined to be 210 cm, a range sufficient to contain all neutral current events, as verified by our calibration data.

Figure 3a is a schematic representation of a neutrino event in the target portion of our detector. A muon may not have sufficient range for identification in the target if its angle relative to the neutrino direction is greater than  $\theta_{max}$ , which depends on the vertex position of the interaction. Charged current events of this type can be removed by a cut on  $y_{NC} = E_{vis}/E(r)$  by employing the kinematical relations between the neutrino energy, the lepton scattering angle and y.  $E_{vis}$  is the observed hadron energy of the interaction, while  $E(r)$  is the neutrino energy predicted from the dichromatic beam at a given radius. The cut on the event sample requires that

$$y_{NC} < y_{cut} \equiv \frac{E(r)\theta_{max}^2}{2M_p + E(r)\theta_{max}^2},$$

where  $\theta_{max} = \arctan \{ (R-r)/L_{cut} \}$ , with  $R = 60$  inches.

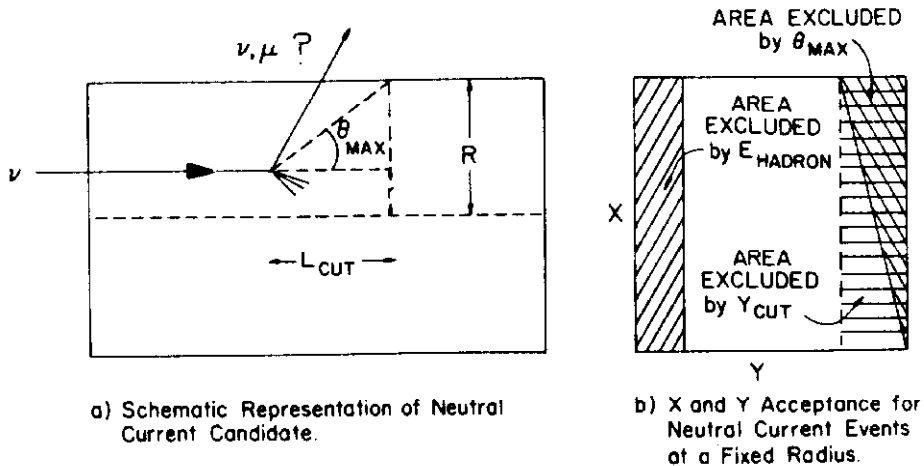


Figure 3.

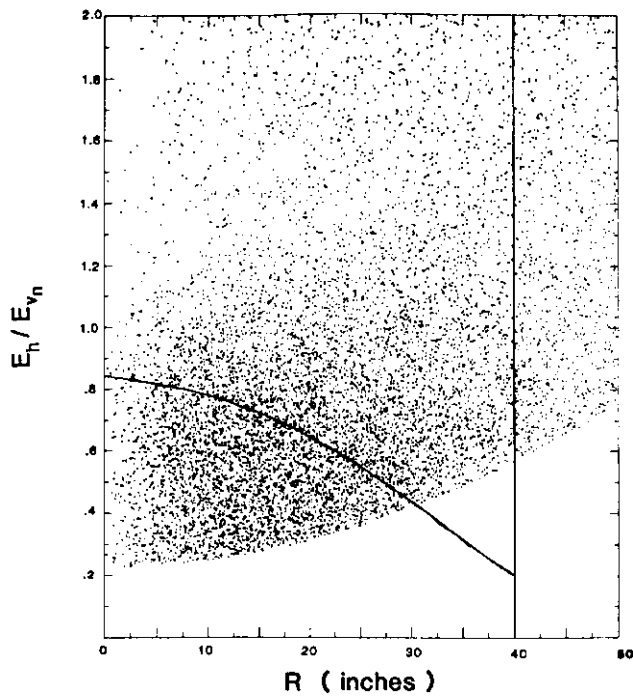
Figure 3b shows schematically, for a fixed radius, the regions in x and y excluded by the  $y_{\text{cut}}$  and the minimum energy requirement. Figure 4 is a scatter plot of events in the  $y_{\text{NC}}$ -radius plane.

Figures 2 and 5 show the event length distribution with and without the  $y_{\text{cut}}$ . After the cut on  $y_{\text{NC}}$  is applied to all events, the length cut at 210 cm gives a much better separation of neutral current and charged current events. Since our event sample is large, this loss of events is not a very severe penalty.

Events with  $y_{\text{NC}} < y_{\text{cut}}$  and  $L < L_{\text{cut}}$  were assumed to include all neutral current events. The remaining charged current contamination in this region is estimated using a Monte Carlo calculation normalized to the number of events with length between 210 and 310 cm. The shape of this calculation agrees well with the data. The contamination due to charged currents is reduced to 5.5% for neutrinos and 2.3% for antineutrinos. To assure that the charged and neutral current events came from the same x-y regions, the charged current events were required to pass the identical criteria as the neutral current events (after correcting for the muon ionization contribution to the hadronic energy) with the exception that the length requirement was  $L > L_{\text{cut}}$ .

In applying the  $y_{\text{NC}}$  cut to the data shown in Figs. 2 and 4, we used the expected neutrino energy for neutrinos originating from pion decay. The use of this pion neutrino energy to calculate  $y_{\text{NC}}$  removes the majority of events due to neutrinos originating from kaon decays since pion neutrinos have roughly half the energy of kaon neutrinos. The remaining background from kaon neutrino neutral current events with small hadronic energy was subtracted using Monte Carlo calculations. The number of such kaon neutrino events surviving the  $y_{\text{cut}}$  is rather small. Table I shows the number of events at various stages of the analysis.

200 GeV Neutrinos



200 GeV Antineutrinos

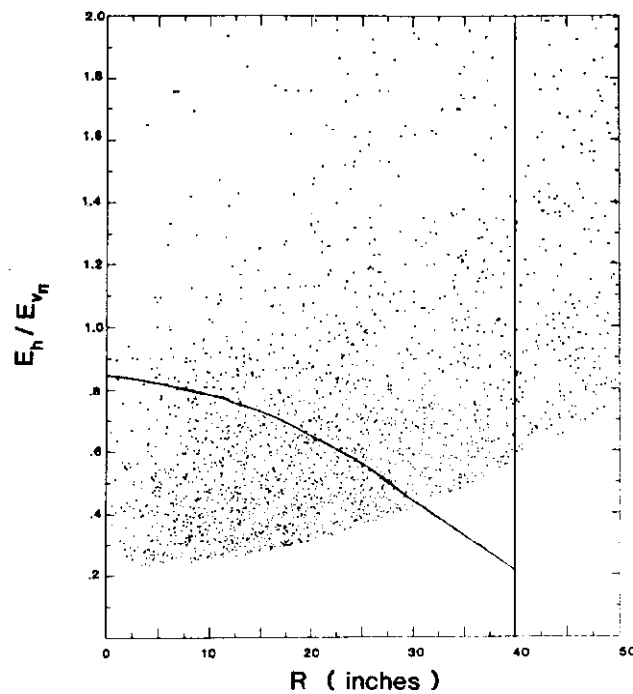


Figure 4.  $y = E_H/E_\nu$  versus radius distribution for the data shown in Figure 2(a). The low  $y$  behaviour of the data reflects the 20 GeV energy requirement. The superposed lines indicate the  $y_{NC} < y_{cut}$  and the  $r < 40$  inches cuts.

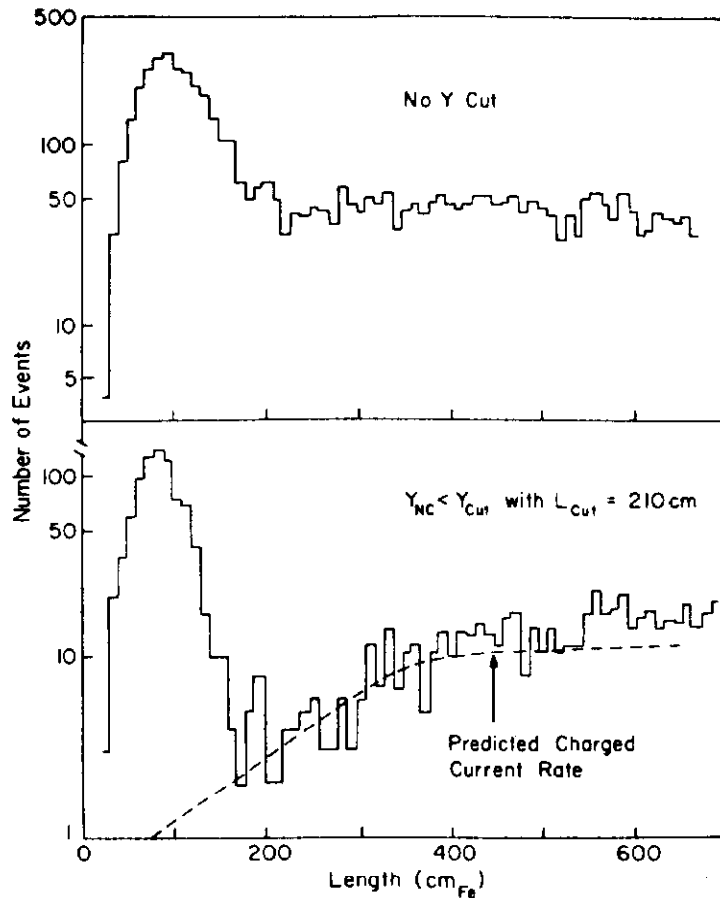


Figure 5. Length distribution for neutrino events (see Fig. 2). The charged current Monte Carlo prediction is also indicated.

	Number of Events	
	Neutrinos	Antineutrinos
Hadronic Energy Trigger, $r < 40$ inches, $E_H > 20$ GeV	32316	7455
$y < y_{cut}$	13950	3760
Pion Neutrino Events	10340	3381
$L < L_{cut}$	2514	961
$L > L_{cut}$	7826	2420
Kaon Neutrino Events	3610	379
$L < L_{cut}$	1029	131
$L > L_{cut}$	2581	248

Table II shows the remaining corrections to the neutral current event sample for pion neutrino events. Due to the limited hadron energy of the pion neutrino events the contamination due to electron neutrino charged current interactions originating from neutrinos produced in  $K_{e3}$  decays, which our apparatus and analysis techniques misidentify as neutral current events, has been substantially reduced by the use of the  $y_{cut}$ . The final event population was determined by applying this  $y_{cut}$  correction as well as corrections due to wide band neutrinos, cosmic ray contamination, neutral current events where a  $\pi$  or a  $K$  in the hadronic shower decays and gives a muon causing them to be misidentified as charged current events, and other minor corrections.

Rather than calculating cross sections, in order to determine the ratios  $R_{-}$  and  $R_{+}$ , we calculated quantities proportional to the cross sections, i.e. the number of events divided by the integrated flux of incident neutrinos or antineutrinos.

TABLE II

Corrections to Neutral Current Events		
	Neutrinos	Antineutrinos
Events	10340	3381
$E_H$ Cut	20 GeV	20 GeV
WBB and Cosmic Rays	-1.3%	-5.0%
CC Background	-5.5%	-2.3%
$K_{e3}$ Background	-1.1%	-0.5%
$\pi/K$ Decay in Shower	+0.1%	+0.1%
Other Corrections	+0.2%	+0.4%
( $\nu_K$ Allowance)	(-9.4%)	(-5.2%)
Total	-7.6%(-17.3%)	-7.3%(-12.5%)

Events with hadronic energies larger than the maximum possible energy that a pion neutrino can have can be uniquely identified as kaon neutrino events. We analyzed this kaon neutrino event sample in a completely analogous manner.

Combining both the pion and kaon neutrino results we find that

$$R_{-} = 0.246 \pm 0.016 \quad \text{and} \quad R_{+} = 0.308 \pm 0.007$$

Figure 6 shows these ratios, for the pion neutrino sample, as functions of the neutrino energy. The ratios show no significant dependence on the neutrino energy or on  $y$  (Ref. 7).

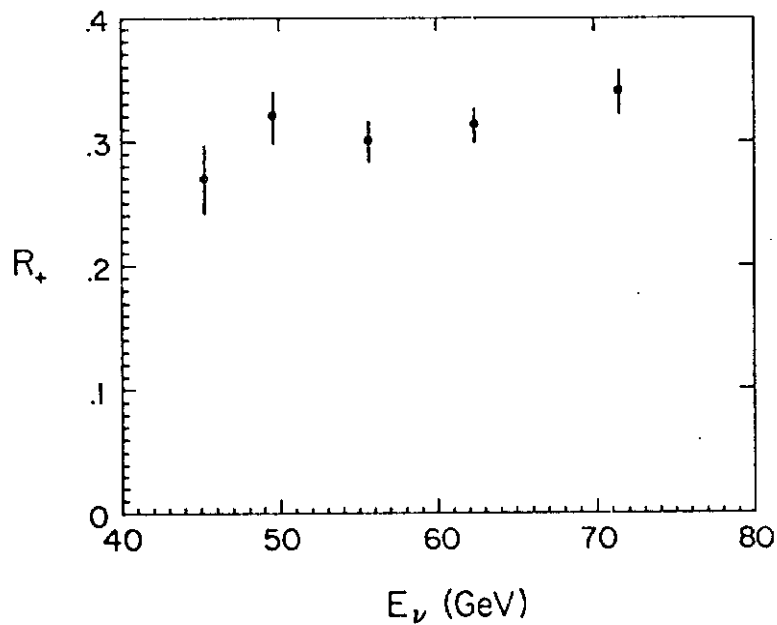
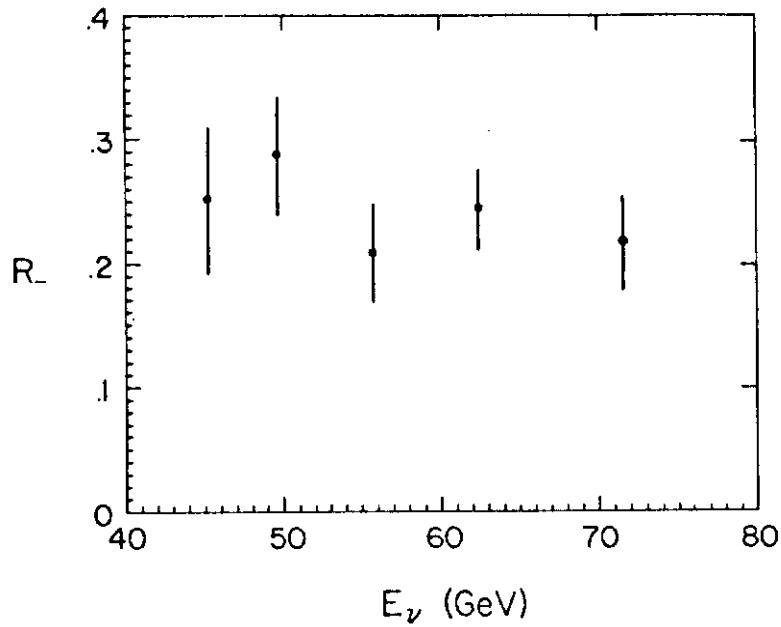


Figure 6.  $R_-$  and  $R_+$  versus mean neutrino energy for the pion data sample after corrections.

Before obtaining  $\sin^2\theta_w$  it is necessary to include additional corrections for the contribution of the strange and charmed sea quarks (to  $R_+$ ), the small difference between the neutrino and antineutrino energy spectra, and the small excess neutron content of our iron target. The sea correction, for the results reported here, has been evaluated in a Monte-Carlo calculation utilizing Buras-Gaemers<sup>8</sup> structure functions and does not include the effects of charm excitation (slow rescaling). These corrections amount to +2.8% for  $R_-$  and +4.1% for  $R_+$ .

Using these corrected ratios we obtain the following values for  $\rho$  and  $\sin^2\theta_w$  :

$$\rho = 1.0054 \pm 0.024 \text{ and}$$

$$\sin^2\theta_w = 0.253 \pm 0.026 .$$

Figure 7 shows the confidence regions in the  $\rho \sin^2\theta_w$  plane. If we

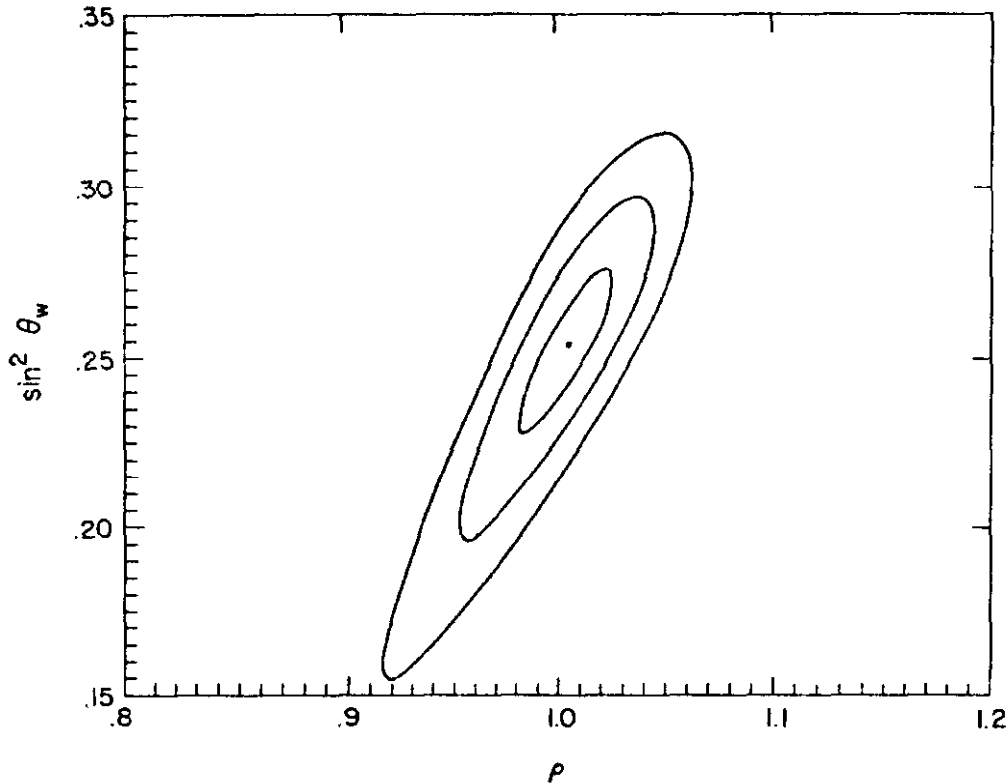


Figure 7. 1 $\sigma$  contours in the  $\sin^2\theta_w - \rho$  plane. The innermost contour corresponds to the 39.4% confidence level.

fix the parameter  $\rho$  to be exactly equal to 1, we then obtain for

$$\sin^2\theta_w = 0.248 \pm 0.012 \quad (\text{statistical error}) .$$

These results are preliminary for the following two reasons :  
1. The corrections due to the strange/charmed sea were evaluated using Buras-Gaemers structure functions and do not include slow rescaling. We are currently evaluating these corrections using structure functions extracted<sup>4</sup> from our experiment. ii. Radiative corrections<sup>9</sup> have not been included. We are also evaluating radiative corrections at this time. Preliminary results from this program indicate that  $\sin^2\theta_w$  decreases by approximately 0.01. We have only quoted statistical errors; a careful evaluation of

systematic errors is also under way. Our preliminary estimate of our systematic uncertainties is 0.015 in the value of  $\sin^2\theta_w$ .

Our value for  $\sin^2\theta_w$ , while consistent with other reported<sup>10</sup> values from neutrino-nucleon scattering, tends to be higher than the world average. The same is also true if we compare our measurement to the values of  $\sin^2\theta_w$  obtained from the measurements of the masses of the  $W^\pm$  and  $Z^0$  in  $p\bar{p}$  collisions. Our measured value of  $\sin^2\theta_w$  is higher than 0.212, the value predicted by SU(5) GUTS ( assuming that  $\Lambda_{\overline{MS}} = 0.24$  GeV).

#### REFERENCES

1. G. Arnison et al., Phys. Lett. 122B, 103 (1983); G. Arnison et al., Phys. Lett. 126B, 398 (1983); M. Banner et al., Phys. Lett. 122B, 476 (1983); P. Bagnaia et al., Phys. Lett. 129B, 130 (1983).
2. W.J. Marciano and A. Sirlin, Phys. Rev. Lett. 46, 163 (1980).
3. B.C. Barish et al., Proceedings of the 9th SLAC Summer Institute of Particle Physics, Stanford, 1981, A. Mosher ed., p. 641 (1982); R.E. Blair, Ph. D. thesis (1982), California Institute of Technology (unpublished); R.E. Blair et al., Fermilab Report Pub-83/26-Exp, 1983 (to be submitted to Nucl. Instr. and Methods).
4. D.B. McFarlane et al., contributed paper to International EPS Conference, Brighton, England, July 1983; R.E. Blair et al., Phys. Rev. Lett. 51, 343 (1983).
5. For a review see: J.E. Kim et al., Rev. Mod. Phys. 53, 211 (1981).
6. E.A. Paschos and L. Wolfenstein, Phys. Rev. D7, 91 (1973). P.Q. Hung and J.J. Sakurai, Phys. Lett. 63B, 295 (1976).
7. M.H. Shaevitz et al., Proceedings of Neutrino-81, International Conference on Neutrino Physics and Astrophysics, Hawaii, 1981, R.J. Cence ed., Vol. I, p. 311; R. Messner, Proceedings of 16th Rencontre de Moriond, 1981, J. Tran Thanh Van ed., Vol. I, p. 341.
8. A.J. Buras and K.J.F. Gaemers, Nucl. Phys. B132, 249 (1978).
9. A. Sirlin and W.J. Marciano, Nucl. Phys. B189, 442 (1981); J.F. Wheeler and C.H. Llewellyn Smith, Nucl. Phys. B208, 27 (1982); E.A. Paschos and M. Wirbel, Nucl. Phys. B194, 189 (1982).
10. See the contributions by C. Geweniger and B. Borgia in these proceedings; also Ref. 5.